European Polymer Journal 44 (2008) 3529–3534

Contents lists available at ScienceDirect

European Polymer Journal

journal homepage: www.elsevier.com/locate/europolj

Macromolecular Nanotechnology

Characterization of the self-assembly process of hydrophobically modified dextrin

Catarina Gonçalves, Francisco Miguel Gama *

IBB-Institute for Biotechnology and Bioengineering, Centre for Biological Engineering, Universidade do Minho, Campus de Gualtar, 4710-057 Braga, Portugal

ARTICLE INFO

Article history:
Received 10 April 2008
Received in revised form 18 July 2008
Accepted 22 August 2008
Available online 3 September 2008

Keywords:
Dextrin
Nanoparticles
Self-assembly
Hydrophobic domains

ABSTRACT

Hydrophobized dextrin, randomly substituted by long alkyl chain (C_{16}), forms stable hydrogel nanoparticles by self-assembling in water. Hydrophobic chains, distributed along the polymer backbone, promote the formation of hydrophobic microdomains within the nanoparticles. The influence of degree of substitution with hydrophobic chains (DS_{C16}) on nanoparticles size, colloidal stability, density, aggregation number and nanoparticle weight was studied. Size distribution was also evaluated at different pH, urea concentration and ionic strength conditions. As shown by dynamic light scattering and transmission electron microscopy, the particles are spherical having a diameter of about 20 nm. The more substituted polymer forms more densely packed hydrophobic microdomains, such that the colloidal stability (in water and PBS buffer) of nanoparticles is increased. The knowledge of the aggregate building process and the characteristics of the nanoparticles are crucial for the design of drug delivery systems.

1. Introduction

Self-assembled hydrogel nanoparticles have potential biomedical and pharmaceutical application due to their biomimetic properties, i.e., their resemblance to biological macromolecules. Amphiphilicity is one of the important factors for the molecular self-organization in water. Various amphiphilic polymers, such as block copolymers [1–5] and hydrophobized polymers [6,7], have been synthesized and studied. Water-soluble polymers hydrophobically modified with hydrophobes grafted to the side chains have special interest. The hydrophobic chains lead to a self-assembly of the polymer, in water, promoting the formation of microdomains within the hydrogel nanoparticles. The microdomains solubilise therapeutic agents, namely hydrophobic drugs. Therefore, they can be used as drug delivery systems.

The attention of the researchers has mainly focused on the preparation of drug-loaded polymeric nanoparticles by varying the polymer/drug ratio, and analysing the drug loading content, entrapment efficiency and drug release profiles. Less attention has been paid to the aggregate building process and to the characterisation of the aggregates. Such assemblies of amphiphilic macromolecules are of interest both for understanding of supramolecular assembly in nature and for designing new materials in biotechnology and medicine. The size, density and stability of the hydrogel nanoparticles may be controlled by changing the hydrophobic group, and also the degree of substitution [8,9]. Akiyoshi and others developed a variety of nanogels made of hydrophobized polysaccharides such as pullulan, mannan and dextran [10–12].

In this work, dextrin derivatives were used for the preparation of self-assembled hydrogel nanoparticles, a new system reported in a previous work [13]. The hydrophobized polysaccharide form relatively monodisperse and colloidally stable nanoparticles (≈20 nm), in water, upon self-aggregation. The nanoparticles characteristics depend on the polymer concentration, degree of substitution with hydrophobic chains (C_{16}), ionic strength and additives. One of the most fundamental and important structural

* Corresponding author. Tel.: +351 253604 418; fax: +351 253678 986.
E-mail address: fmgama@deb.uminho.pt (F.M. Gama).

0014-3057/$ - see front matter © 2008 Elsevier Ltd. All rights reserved.
doi:10.1016/j.eurpolymj.2008.08.034

parameters of micellar aggregates is the aggregation number, the average number of hydrophobic molecules in a micelle unit [14,15]. The aim of the present work is to study the aggregate building process and the characteristics of the nanoparticles formed. This fundamental information enables us to design a useful nanosized delivery system suitable for carrier of hydrophobic drugs.

2. Experimental part

2.1. Materials

Dextrin-VA-SC_{16} ($dexC_{16}$) was synthesized as described previously [13]. In this work, dextrin-VA with 20 acrylate groups per 100 dextrin glucopyranoside residues (DS_{VA} 20%) was used.

Pyrene (Py) and cetylpyridinium bromide (CPB) were obtained from Aldrich. Pyrene was used after recrystallization. Ultra-pure water (Milli Q) was used for the preparation of aqueous solutions.

2.2. Preparation of self-assembled nanoparticles

Lyophilized $dexC_{16}$ was dissolved in ultra-pure water under stirring, at 50 °C, and then further sonicated for 20 min until a clear solution was obtained. The solution of self-assembled nanoparticles was then filtrated through a 0.20 μm filter and stored at room temperature.

2.3. Size distribution and zeta potential

The size distribution, zeta potential and nanoparticle weight were determined with a Malvern Zetasizer, NANO ZS (Malvern Instruments Limited, UK), using a He–Ne laser (wavelength of 633 nm) and a detector angle of 173°. Size distribution and zeta potential were determined by dynamic light scattering (DLS).

For size distribution measurements, a dispersion of nanoparticles in ultra-pure water or PBS buffer (1 mL) was analysed at 25 °C in a polystyrene cell. The concentration of nanoparticles was adjusted by dilution with ultra-pure water of concentrated nanoparticle dispersion.

The DLS cumulants analysis provides the characterization of a sample through the mean value (*z*-average) for the size, and a width parameter known as the polydispersity, or polydispersity index (PdI). The *z*-average diameter is the mean hydrodynamic diameter, determined from the intensity of scattered light. The fundamental size distribution generated by DLS is an intensity distribution, this can be converted, using Mie theory, to a volume distribution. This volume distribution can also be further converted to a number distribution. In the present work, we will consider the *z*-average as the best approach to the actual nanoparticles size.

For zeta potential measurements, the aqueous solutions of nanoparticles at different pH values were obtained by dissolving $dexC_{16}$ with DS_{C16} 6.1% (0.1 gdL^{-1}) in phosphate-citrate buffer (pH 2.2–8.0). Each sample was analysed in a folded capillary cell. The zeta potential values were calculated using the Smoluchowski equation. Repeated measurements were performed (3 times) and the values reported are average values.

2.4. Static light scattering

Nanoparticle weight was determined by static light scattering (SLS). The intensity of scattered light produced by macromolecules is proportional to the product of the weight–average nanoparticle weight and the concentration of the macromolecule. For molecules that show no angular dependence in the light scattering (when molecules are not large enough to accommodate multiple photon scattering), the relationship between the intensity of scattered light and the molecular weight is given by the Rayleigh equation. In the present study the nanoparticle weight will be evaluated using the follow equation:

$$\frac{KC}{R_\theta} = \left(\frac{1}{NP_w} + 2A_2C\right) \quad (1)$$

NP_w is the weight–average nanoparticle weight, A_2 is the second virial coefficient and C is the sample concentration, K is an optical constant as defined below:

$$K = \frac{2\pi^2}{\lambda_0^4 N_A}\left(n_0\frac{dn}{dc}\right)^2 \quad (2)$$

N_A, Avogadro's constant; λ_0, laser wavelength; n_0, solvent refractive index; dn/dc, differencial refractive index increment.

R_θ is the Rayleigh ratio – the ratio of scattered light to incident light of the sample. The standard approach for weight measurements is to first measure the scattering intensity of the analyte used relative to that of a well described "standard" pure liquid with a known Rayleigh ratio. Toluene was used as standard. The refractive index increment (dn/dc) used in SLS measurements was measured in a differencial refractometer. For the present polymer dn/dc of 0.140 mL g^{-1} was obtained. In the plot of $KC/R\theta$ versus C (known as Debye plot) the intercept is equivalent to $1/NP_w$ and the slope allows the calculation of the second virial coefficient A_2. The second virial coefficient is a property describing the interaction strength between the nanoparticles and the solvent. For samples where $A_2 > 0$, the nanoparticles are stable in solution. When $A_2 = 0$, the nanoparticle–solvent interaction is equivalent to the nanoparticle–nanoparticle interaction and the solvent is described as a theta solvent. When $A_2 < 0$, the nanoparticles are unstable, and aggregate.

A glass cell was used for nanoparticle weight measurements. All dispersions were filtered using disposable 0.20 μm filters. This filtration has a significant effect on the size distribution, reducing the polydispersity index. A larger PdI being observed when a 0.45 μm filter was used.

2.5. Transmission electron microscopy

For visualization by transmission electron miscroscopy (50 kV; Zeiss EM 902C), nanoparticles were adsorbed to glow-discharged carbon-coated collodion film on 400-mesh copper grids. Grids were washed with deionized water and stained with 0.75% uranyl acetate.

2.6. Fluorescence spectroscopy

Fluorescence measurements were performed on a VARIAN Cary Eclipse fluorescence spectrofluorometer using a quartz cell. Experiments were performed with Py as a fluorescent probe (1×10^{-6} M) and CPB as a quencher (0.01–0.1 mM). A stock solution of CPB (1 mM in methanol) was prepared, and aliquots of this solution were added to empty flasks in the amount required for the final CPB concentration. Methanol was evaporated and then a polymer solution with a 0.3 g dL^{-1} concentration, prepared in 1×10^{-6} M Py, was added to each flask. The mixtures were left to equilibrate under mild shaking for 24 h. The pyrene spectra were obtained using an excitation wavelength of 337 nm, and recording the emission over the range 350–500 nm, at a scan rate of 20 nm min^{-1}. The slit width was set at 20 nm for the excitation and 2.5 nm for the emission.

3. Results and discussion

3.1. Size of the dexC_{16} self-aggregates

Several samples of dexC_{16} were prepared, as reported previously, with DS_{C16} (C_{16} groups per 100 dextrin glucopyranoside residues) of 3.4, 4.8, 6.0, 8.8 and 10.0%. The size and size distribution of the self-assembled hydrogel nanoparticles in aqueous medium were measured by DLS. Fig. 1 shows the particle size of the samples at different polymer concentrations. The concentration range is above critical micelle concentration (≈0.0008 g dL^{-1}) and below the solubility limit (≈1 g dL^{-1}) [13].

The average of the obtained z values, for samples with DS_{C16} 4.8, 6.0, 8.8 and 10.0%, was 20.0 ± 1.2, 19.6 ± 1.1, 22.7 ± 1.1 and 22.6 ± 0.7 nm, respectively (±confidence interval at 95%), with corresponding average polydispersity index of 0.390, 0.354, 0,559 and 0.306. These results indicate that the particle size of the self-assembled hydrogel nanoparticles is only slightly influenced by the DS_{C16} or polymer concentration.

As can be seen in Fig. 2, the size distribution of hydrophobized polysaccharide in water, upon self-aggregation, is relatively monodisperse. The intensity distribution is rather influenced by the presence of larger particles, while the volume distribution provides a better approach to characterize the more representative population.

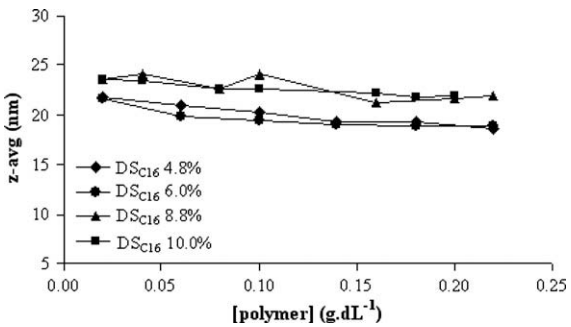

Fig. 1. Z-average analysis of self-assembled hydrogel nanoparticles with DS_{C16} 4.8, 6.0, 8.8 and 10.0%.

In addition, the self-assembled nanoparticles were observed using transmission electron microscopy (TEM). Fig. 3 reveals spherical nanoparticles with a predominant population with diameters of about 20 nm for dexC_{16} with DS_{C16} 8.8%. The TEM results are in good agreement with DLS results presented above.

3.2. Aggregation number (Hydrophobic groups in the microdomains)

Fluorescence quenching is a common method for the measurement of the aggregation number. The method is based on the quenching of a probe's emission using a specific quencher (Q). Both probe and quencher should have a high affinity for the nanoparticles. Considering a well-defined but unknown microdomains concentration [MD] and a concentration of quencher [Q], selected such that it resides exclusively in the nanoparticles, then Q will be distributed among the available nanoparticles. If a fluorescent molecule P, which is also entirely associated with nanoparticles, is now added to the system, P will partition between nanoparticles containing Q and the "empty" nanoparticles. A Poisson distribution of the P and Q among the nanoparticles may be assumed. If P is fluorescent only when it occupies an empty nanoparticle, then the measured ratio of fluorescence intensities (I/I_0), obtained in the presence (I) or absence (I_0) of Q, is related by the equation:

$$\left(\frac{I}{I_0}\right) = \exp\left\{-\frac{[Q]}{[MD]}\right\} \Longleftrightarrow \ln\left(\frac{I_0}{I}\right) = \frac{[Q]}{[MD]} \tag{3}$$

In this work, CPB was used as the pyrene quencher. We used a low concentration of CPB (0.01–0.1 mM) to minimize a possible aggregation of this pyridinium surfactant (critical micelle concentration of CPB is about 0.6 mM). For the quenching experiments, the polymer concentration used was in the range where saturation with pyrene takes place, that is, where a constant value for the ratio I_3/I_1 is reached [13].

The plots of $\ln(I_0/I)$ versus [Q] give straight lines (Fig. 4) allowing the calculation of [MD] and then N_{agg}, according to Eq. (4):

$$N_{agg} = \frac{c_H}{[MD]} \tag{4}$$

where c_H is the hydrophobic groups concentration, in mM.

The fluorescence quenching study reveals that the hydrophobic microdomains (MD) have a number of alkyl chains that increases with DS_{C16}, from 4 to 18, in the range of the DS_{C16} values analysed (Fig. 5).

The more substituted polymer forms more densely packed hydrophobic microdomains, due to an increase in the number of alkyl chains. However, the nanoparticle diameter is not significantly influenced. The higher N_{agg} of the more substituted material (higher DS_{C16}) probably corresponds to nanoparticles with improved stability, due to the increased hydrophobic interaction on the microdomains. The stability of nanoparticles obtained with DS_{C16} 4.8 and 8.7% was evaluated up to 7 days. Aqueous dispersions (0.1 g dL^{-1}) were stored in the DLS polystyrene cell, at room temperature. The size distribution was constant,

a

			Diam.(nm)	% Intensity	Width (nm)
Z-Average (d.nm):	23.6	Peak 1:	21.8	73.9	10.3
PdI:	0.363	Peak 2:	164	26.1	80.5
Intercept:	0.919	Peak 3:	0.0	0.0	0.0

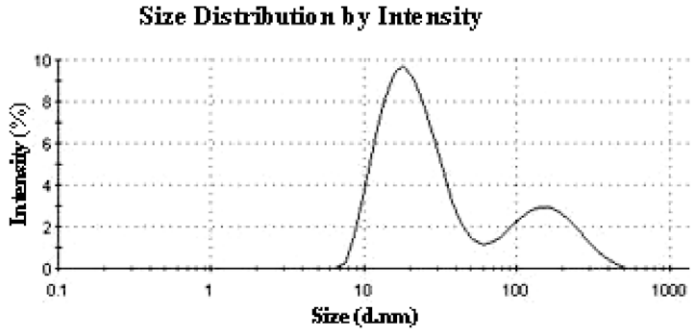

b

			Diam.(nm)	% Volume	Width (nm)
Z-Average (d.nm):	23.6	Peak 1:	13.9	100	7.8
PdI:	0.363	Peak 2:	0.0	0.0	0.0
Intercept:	0.919	Peak 3:	0.0	0.0	0.0

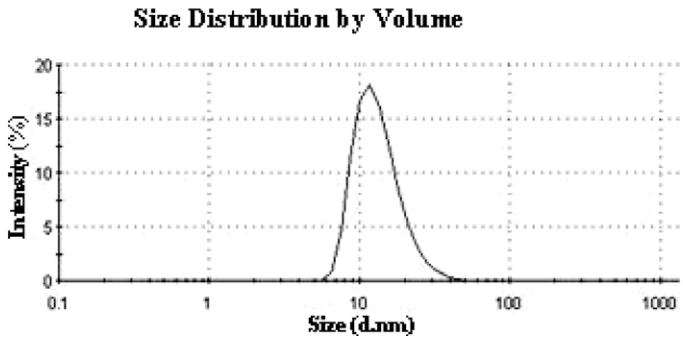

Fig. 2. Size distribution in (a) intensity (%) and (b) volume (%), of aqueous dispersion 0.02 g dL^{-1} of $dexC_{16}$ with DS_{C16} 8.8%.

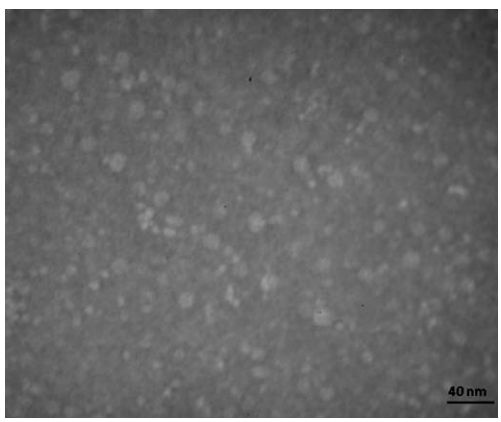

Fig. 3. Transmission electron microscopy of negatively stained nanoparticles with DS_{C16} 8.8%.

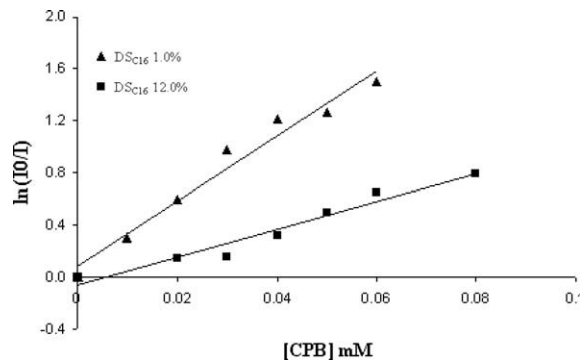

Fig. 4. Variation of $\ln(I_0/I)$ as a function of CPB concentration, for different degree of substitution of the polymer.

for DS_{C16} 8.7%, with low polydispersity index (<0.5), up to 7 days. In the case of DS_{C16} 4.8% some aggregates are detected in the first day of the assay (≈500 nm), but the main peak was conserved. The stability was also evaluated for DS_{C16} 8.7% in PBS (0.1 g dL^{-1}). The sample was highly stable, since no aggregates were detected and the low polydispersity index was also conserved. Indeed, as expected, the more substituted $dexC_{16}$ forms more compact hydrophobic microdomains, such that the colloidal stability of nanoparticles is increased.

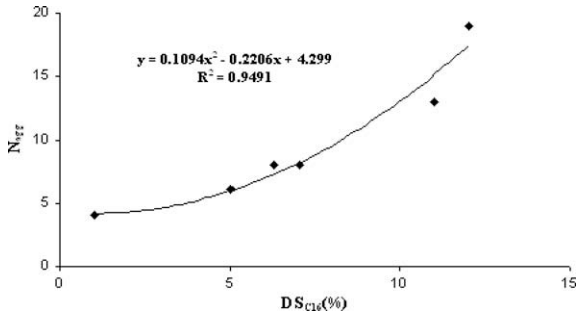

Fig. 5. Aggregation number (N_{agg}) of the microdomains as a function of the degree of substitution, for a polymer concentration of 0.3 g dL^{-1}.

3.3. Weight of the dexC_{16} self-aggregates (SLS assays)

The nanoparticle weight (NP_w) and the second virial coefficient (A_2) of the dexC_{16} self-aggregates were studied, for different degrees of substitution, using the Debye plot. The second virial coefficient (A_2) of the nanoparticles is positive, revealing stability in aqueous medium. The value obtained, divided by the molecular weight of a single polymer chain, provide the number of polymer (dexC_{16}) molecules within a nanoparticle. Thus, using the aggregation number determined by quenching experiments, a comprehensive characterization of nanoparticle is possible, namely the estimation of the number of polymer molecules (molecules/NP) and hydrophobic moieties per nanoparticle (C_{16}/NP), number of hydrophobic molecules within one hydrophobic microdomain (N_{agg}) and number of hydrophobic microdomains (MD/NP). The results are presented in Table 1. As shown, dexC_{16} used for the nanoparticle weight determination has not the same DS_{C16} as one used for N_{agg} determination (see Fig. 5). Therefore, the values of N_{agg} used for nanoparticle characterization (Table 1) were obtained using the trend line shown in Fig. 5.

The nanoparticle weight determination (by SLS) allows an estimation of the number of polymer molecules, per nanoparticle, in the range 151–216 (Table 1), depending on the degree of substitution.

The N_{agg} value has been calculated under the assumption that all hydrophobes are involved in hydrophobic microdomains. This assumption might be true for polymers with higher degrees of substitution [8], where the density of the side alkyl chains is high enough. Therefore, N_{agg} corresponds to the maximum number of hydrophobes that can exist within microdomain.

From the experimental hydrodynamic radius (R_H) and NP_w values, one can calculate the average polymer density (φ_H) within a nanoparticle, as defined by Eq. (5), where N_A is Avogadro's number.

$$\phi_H = \left(\frac{NP_w}{N_A}\right)\left(\frac{4}{3}\pi R_H^3\right)^{-1} \quad (5)$$

The average polymer density, for samples with DS_{C16} 4.8, 6.0, 8.8 and 10.0%, was 0.14, 0.17, 0.11 and 0.15 g mL^{-1}, respectively. These results indicate that the nanoparticles have about 85–90 wt% of water; they may be considered hydrogel-like structures.

3.4. Influence of pH, urea and ionic strength

The magnitude of the zeta potential gives an indication of the stability of the colloidal system. If particles in a suspension have a large zeta potential value, negative or positive, then they will repeal each other and the particles do not aggregate. However, if the particles have a low zeta potential value (close to zero), then there is no electrostatic force to prevent the particles to aggregate. The most important factor that affects zeta potential is pH. The variation of hydrodynamic diameter and zeta-potential of nanoparticles with the pH was studied.

Fig. 6 shows that the nanoparticles size is not sensitive to the medium pH. In the pH range studied, the zeta potential is almost constant and close to zero. Indeed, the polymer is made of glucose, and the hydroxyl glucose residues have a high pK_a (12.35), and thus the material is expected to be poorly ionized in the analysed pH range. Although the low zeta potential, the nanoparticles are stable. The stability can be attributed to the solvation forces. Typically, solvation forces are ignored in colloidal analysis, because they are difficult to access and quantify. It has been noted that solvation forces can be comparable to, or greater than, van der Waals forces [16].

In order to further understand the nature of the associations exhibited by dexC_{16} in aqueous medium, the effects of urea and salt (NaCl) on nanoparticle size was studied.

Urea can produce twofold effects: firstly, urea may break intra-molecular hydrogen bond, an effect that may lead to the uncoiling of dextrin molecules, which would assume a more extended conformation. Secondly, urea can severely disturb the hydrophobic interactions. It was found that particle size slightly increases with the urea concentration. Using DS_{C16} 8.8% (0.1 g dL^{-1}), the nanoparticles size increase from 25.8 to 31.3 nm, corresponding to an urea concentration up to 7 M. Thus, urea seems to perturb the hydrophobic interactions inducing the nanoparticles to "swell", although it is noticeable that the size increase is not dramatic. Indeed, the driving force for hydrophobic association in aqueous systems is partially attributed to the need for the hydrophobic moieties to minimize the surface area of contact with water, and consequently minimize the amount of water that must be "structured" in order to solubilise them. The addition of urea to aqueous solutions disrupts the structuring ability of water, thereby weakening the hydrophobic interactions in the solution [17]. Therefore, urea may hinder the formation of hydrophobic domains, although it does not prevent the formation of nanoparticles.

The effect of NaCl concentration on the hydrodynamic diameter of nanoparticles obtained with DS_{C16} 9.0% (0.1 g dL^{-1}) was also studied. An increase of the average particle size, in the same range as observed with urea, may be observed. Nanoparticles size increase from 23.7 to 35.5 nm, corresponding to NaCl concentration in the range 0–0.6 M. Since nanoparticles bears a rather low charge, considering the zeta potential, the size increase is not likely to arise from the double layer compression and subsequent aggregation.

The interaction forces between colloidal nanoparticles determine the dispersion and stability of their suspensions.

Table 1
Nanoparticles characterization with different DS

DS_{C16} (%)	C_{16}/molecule[a]	Mw $dexC_{16}$ (Da)[a]	NP_w[b] (kDa)	A_2 mL mol/g[2b]	Molecule/NP	C_{16}/NP	N_{agg} calc[c]	MD/NP	Molecules/MD
3.4	0.4	2231	336	4.75e-4	151	60	5	12	13
4.8	0.6	2278	346	4.95e-4	152	91	6	15	10
6.0	0.8	2318	411	3.82e-4	177	142	7	20	9
8.8	1.1	2412	418	4.93e-4	173	190	11	17	10
10.0	1.3	2452	530	2.53e-4	216	281	13	22	10

[a] $M_W(dexC_{16}) = 2106 + (\frac{\%DS_{C16}}{100} \times 258.1) + (\frac{\%DS_{VA}}{100} \times 54.1)$, assuming M_w(dextrin) = 2106 Da, determined previously by chromatography.
[b] Determined by static light scattering.
[c] Determined by: $N_{agg}\text{calc} = 0.1094 \times (DS_{C16})^2 - 0.2206 \times DS_{C16} + 4.299$ (trend line equation in Fig. 5).

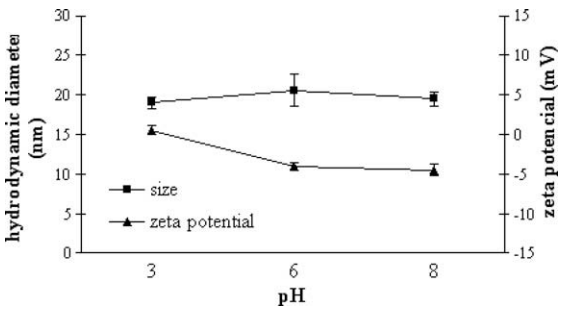

Fig. 6. Particle size and zeta potential of nanoparticles with DS_{C16} 6.1% (0.1 g dL^{-1}) as a function of solution pH.

Electrostatic, van der Waals, depletion, and solvation forces exist between solid particles suspended in a liquid. However, for nanoparticles, the absolute and relative magnitudes of these forces are not well-known. It is difficult to measure forces acting upon nanoparticles, experimentally.

The general conclusion that may be drawn from these results is that the nanoparticles have a slightly higher size when prepared in buffer (irrespective of the pH), in the presence of a salt or urea (irrespective of the concentration). The rather high stability of these nanoparticles must be remarked.

4. Conclusions

In the present study we evaluated the influence of the degree of substitution on the self-assembly process of a hydrophobized dextrin polymer, $dexC_{16}$. The size of self-assembled hydrogel nanoparticles was evaluated as a function of DS_{C16}. The nanoparticles size is only slightly influenced by DS_{C16} or polymer concentration. The fluorescence quenching study reveals that the more substituted polymer forms more densely packed hydrophobic microdomains, such that colloidal stability (in water and PBS) of nanoparticles is increased. The nanoparticles are stable in the presence of urea and at different pH and ionic strength. Small size, low density and high stability of the nanoparticles obtained can promote a stable entrapment of bioactive and hydrophobic molecules, and allow them to circulate in the blood long enough to reach the desired therapeutic effects.

Acknowledgments

This research was supported by Fundação para a Ciência e a Tecnologia under Grant SFRH/BD/22242/2005 and POCTI/BIO/45356/2002.

References

[1] Chen C, Yu CH, Cheng YC, Yu PHF, Cheung MK. Eur Polym J 2006;42(10):2211–20.
[2] Liang H, Chen C, Chen S, Kulkarni AR, Chiu Y, Chen M, Sung H. Biomaterials 2006;27:2051–9.
[3] Chen C, Yu CH, Cheng YC, Yu PHF, Cheung MK. Biomaterials 2006;27:4804–14.
[4] Gaucher G, Dufresne MH, Sant VP, Kang N, Maysinger D, Leroux JC. Journal of Controlled Release 2005;109:169–88.
[5] Letchford K, Burt H. Eur J Pharm Biopharm 2007;65:259–69.
[6] Na K, Park K, Kim SW, Bae YH. J Control Release 2000;69:225–36.
[7] Roux M, Perly B, Djedaini-Pilard F. Eur Biophys J 2007;36:861–7.
[8] Nichifor M, Lopes S, Bastos M, Lopes A. J Phys Chem B 2004;108:16463–72.
[9] Akiyoshi K, Sunamoto J. Supramol Sci 1996;3:157–63.
[10] Akiyoshi K, Deguchi S, Moriguchi N, Yamaguchi S, Sunamoto J. Macromolecules 1993;26:3062–8.
[11] Akiyama E, Morimoto N, Kujawa P, Ozawa Y, Winnik FM, Akiyoshi K. Biomacromolecules 2007;8:2366–73.
[12] Kim I, Jeong Y, Kim S. Int J Pharm 2000;205:109–16.
[13] Gonçalves C, Martins JA, Gama FM. Biomacromolecules 2007;8:392–8.
[14] Turro NJ, Yekta A. J Am Chem Soc 1978;100(18):5951–2.
[15] Vorobyova O, Lau W, Winnik MA. Langmuir 2001;17:1357–66.
[16] Fichthorn KA, Qin Y. Ind Eng Chem Res 2006;45:5477–81.
[17] Philippova OE, Volkov EV, Sitnikova NL, Khokhlov AR. Biomacromolecules 2001;2:483–90.